ASEAN
Journal of Scientific and Technological Reports
Online ISSN:2773-8752

Research article

Preparation and Characterization of Sulfonated CaO Catalyst for Biodiesel Production from Waste Cooking Oil

Chatchawin Dulymahakamtorn[1], Rattana Jariyaboon[2], Prawit Kongjan[3], Tanakorn Chantasuban[4], and Saowapa Chotisuwan[5*]

[1] Department of Science, Faculty of Science and Technology, Prince of Songkla University, Pattani, 94000, Thailand
[2] Department of Science, Faculty of Science and Technology, Prince of Songkla University, Pattani, 94000, Thailand
[3] Department of Science, Faculty of Science and Technology, Prince of Songkla University, Pattani, 94000, Thailand
[4] Department of Science, Faculty of Science and Technology, Prince of Songkla University, Pattani, 94000, Thailand
[5] Department of Science, Faculty of Science and Technology, Prince of Songkla University, Pattani, 94000, Thailand
* Correspondence: saowapa.c@psu.ac.th

Citation:
Dulymahakamtorn, C.; Jariyaboon, R.; Kongjan, P.; Chantasuban, T.; Chotisuwan, S. Preparation and characterization of sulfonated CaO catalyst for biodiesel production from waste cooking oil. *ASEAN J. Sci. Tech. Report.* **2025**, *28*(1), e255558. https://doi.org/10.55164/ajstr.v28i1.255558.

Article history:
Received: August 18, 2024
Revised: October 17, 2024
Accepted: November 9, 2024
Available online: December 14, 2024

Abstract: Biodiesel production depends on raw materials. Low-quality oils, such as cooking oil, crude palm oil, and sludge oil, are used to reduce costs, and they contain free fatty acids (FFA) and water. Soap can be produced when using the alkaline catalyst during transesterification. In this work, the sulfonation method prepared the esterification of waste cooking oil by sulfonated CaO as a bifunctional catalyst. The sulfonated CaO catalysts were characterized by X-ray diffraction spectroscopy (XRD), Fourier transform infrared spectroscopy (FTIR), temperature-programmed desorption of carbon dioxide and ammonia (TPD), BET surface area, and scanning electron microscopy (SEM). It was observed that the specific surface area, pore volume, and pore diameter of the CaO increased after being sulfonated with a 2 M sulfuric acid solution. It showed a high total surface acidity and basicity, 7.22 and 3.86 mmol/g, respectively. The optimal FFA conversion (84.94 %) from the waste cooking oil was acquired at a reaction temperature of 65 ˚C, a 9:1 MeOH: Oil molar ratio, and 5 wt% catalyst loading for a 3 h reaction time. The 2 M sulfonated CaO catalyst can be reused twice with a high FFA conversion without further treatment under optimized reaction conditions. The 2 M sulfonated CaO catalyst has potential treatment for biodiesel production from high-FFA oils due to its lower production cost and high catalytic activity.

Keywords: Waste cooking oil; Esterification; Sulfonated catalyst; Biodiesel, Calcium oxide

1. Introduction

Biodiesel is a clean alternative to diesel fuel. The raw ingredients for biodiesel manufacturing comprise vegetable oils, recycled vegetable oils such as palm, soybean, sunflower oils, and animal fats. The oxygen content in biodiesel facilitates more complete combustion than diesel fuel, leading to diminished black smoke and carbon monoxide emissions, reducing air pollution [1]. Typically, oils and fats undergo transesterification to generate biodiesel. When triglycerides in oils react with alcohol, biodiesel, and glycerol are made as byproducts [2]. A suitable catalyst helps along this reaction. The manufacture of biodiesel through transesterification can utilize bases, acids, and enzymes as

catalysts [3]. There are two categories of base-type catalysts: heterogeneous and homogeneous catalysts. The homogeneous catalyst employed in the transesterification reaction is sodium hydroxide, usually used in biodiesel production, such as B100 or pure biodiesel on an industrial scale in Thailand. The homogenous base catalyst exhibited superior speed to the acid catalyst [4]. Nonetheless, substantial water is required to eliminate the catalyst from the biodiesel post-reaction [5]. Using a base catalyst in biodiesel production may induce undesirable side reactions, including saponification, which diminishes biodiesel yield and complicates the separation and purification processes [6-8].

To mitigate these adverse effects, an acid-base catalyst, also called a bifunctional catalyst, has garnered considerable attention. This catalyst can react with the esterification of free fatty acids and the transesterification of triglycerides contained in oil [9]. Both acidic and base-active sites work on its surface. Therefore, it is not affected by the amount of water in raw materials or the amount produced during biodiesel production [10]. Thus, using a bifunctional catalyst, these unwanted reactions to produce soap reactions or saponification can be addressed to make the process more feasible. Therefore, it can effectively reduce the cost of biodiesel production. In addition, this type of catalyst can modify the characteristics necessary for reducing the effects due to the presence of free fatty acids and water in low-quality raw materials during biodiesel production through the transesterification of triglycerides [11]. CaO is a common solid base heterogeneous catalyst for biodiesel production by transesterification due to its relatively low-cost production and high basicity and activity [8-9]. However, the CaO catalyst is not suitable for low-grade oil feedstock. In this case, there are modifications of CaO to contain both acidic and basic sites or bifunctional catalysts. Some modified basic or acidic oxide heterogeneous catalysts have been reported, such as a sulfonated carbon-based catalyst, modified CaO with ZrO and TiO_2, sulfated ZrO, ZnO/CaO, and TiO_2/CaO to catalyze biodiesel production [1-2, 5, 8-12]. Treating changed metal oxides with diluted sulfuric acid is a simple method to create sulfated or high-acidity sulfonated catalysts [12–15]. Syazwani and co-workers [13-14] prepared a bifunctional, sulfated CaO from a waste angle wing shell (CAWS) treated by sulfonation with 3-11 M H_2SO_4. They used it to catalyze the esterification of palm fatty acid distillate (PFAD) to biodiesel. They observed the optimum condition by using 7 M H_2SO_4-treated CAWS. Istadi and co-workers reported a 2 M H_2SO_4 treatment for sulfated ZnO, which demonstrated good performance in the transesterification of soybean oil [12]. Valizadeh and co-workers [15] also reported a two-step technique that involved pretreatment and sulfonation with 0.5 M H_2SO_4 for Al_2O_3, MgO, ZrO_2, and TiO_2. The authors attributed the high potential for ester production of sulfonated Ti-SO_4 and Zr-SO_4 to the well-distributed Bronsted acid sites formed by –SO_3H groups [15].

Those modified CaO catalysts were derived from natural CaO sources or biobased CaO, which may not be cost-effective on an industrial scale. Thus, this work aimed to prepare a low-cost, bifunctional heterogeneous sulfonated CaO catalyst by using a diluted sulfuric acid solution, characterization by various techniques to obtain chemical, physical, crystal phase, morphology, and acidity properties of the catalyst, and then the catalytic activity for biodiesel production from waste cooking oil was investigated.

2. Materials and Methods

2.1 Materials

Waste cooking oil (WCO) was collected from a fried chicken restaurant, Charoenpradit Road, Rusamilae, Mueang, Pattani, Thailand. Acetic acid (CH_3COOH) (ACS grade, J.T.Baker, China), methanol (CH_3OH) (ACS grade, Honeywell Burdich & Jackson, Korea), calcium oxide (CaO) (extra pure, Loba Chemie, India), carbon tetrachloride (CCl_4) (AR grade, QRëC, New Zealand), diethyl ether ($(C_2H_5)_2O$) (ACS grade, PanReac AppliChem, Spain), ethanol (C_2H_5OH) (ACS grade, VWR prolabo chemicals, France), n-hexane (C_6H_{14}) (ACS grade, Riedel-de Haën, Germany), iodine (I_2) (AR grade, VWR chemicals, Japan), phenolphthalein ($C_{20}H_{14}O_4$) (AR grade, Ajax Finechem, Australia), potassium hydroxide (KOH) (AR grade, Loba Chemie, India), potassium iodide (KI) (ACS grade, Ajax Finechem, Australia), sodium hydroxide (NaOH) (AR grade, Loba Chemie, India), sodium thiosulfate ($Na_2S_2O_3$) (AR grade, Ana PURE, New Zealand), sulfuric acid (H_2SO_4) (AR grade, Loba Chemie, India). All chemicals except WCO were used as received.

2.2 Catalyst preparation

A low-cost sulfonated CaO catalyst was synthesized by reacting 5 g of CaO powder with 25 mL of 2 M sulfuric acid [12], in contrast to 7 M sulfuric acid [13-14], and stirring for 2 hours at room temperature. Then the

sulfonated/sulfated CaO catalyst was filtered through a vacuum filter and washed with distilled water until the pH of the filtrate was equal to 7 to remove excess acid or sulfate, then dried in the hot air oven at 105 °C for 12 hours [12].

2.3 Catalyst characterization

The sulfonated/sulfated calcium oxide was characterized by X-ray diffraction (XRD) (Empyrean, PANanalytical, Netherlands) using Cu K_α radiation, with a wavelength of 1.5418 Å at 40 kV and 40 mA. The XRD data of samples were recorded in 2θ range varying from 5° to 90°. The surface functional groups of catalyst samples were investigated using Fourier transform infrared spectroscopy (FTIR) (Bruker Tensor 27, United States) scanned at wavenumber 400–4000 cm^{-1}. The specific surface area and pore volume of the synthesized catalyst were investigated by BET (Surface analyzer, ASAP2460, Micromeritics, USA). The catalyst was degassed overnight in a vacuum at 120 °C before analysis, and N_2 adsorption was performed at -196 °C. The total acidity and basicity of catalysts were determined by temperature-programmed desorption of NH_3 and CO_2 (TPD, BEL, BEL CAT II, Japan); the solid sample was heated at 400 °C in an H_2 flow at a rate of 10 °C min^{-1} for 2 hours. Then NH_3 (0.1%) gas was passed through the solid sample for 1 hour after the sample was cooled to 100 °C in helium flow. The quantity of desorbed NH_3 gas from the catalyst during increasing temperature was detected following each TPD operation. A similar method was applied for TPD- CO_2, but CO_2 gas was used instead of NH_3. The morphology of the synthesized catalyst was characterized by scanning electron microscopy (SEM, ThermoFisher Scientific- Phenom ProX, USA) with voltage at 10 kV. The samples were also subjected to energy-dispersive X-ray (EDX, HITACHI, SU3900, Japan) for elemental analysis.

2.4 Esterification of waste cooking oil

WCO was pretreated by heating it to 100 °C for 40 minutes to remove the water and impurities, followed by filtration. The percentage of FFA content in WCO was then determined using acid-base titration. The titration was done by weighing 2.0 g of WCO sample into a 50 mL diethyl ether and ethanol mixture (50% vol), using phenolphthalein as an indicator. Finally, it was titrated with a 0.1 N NaOH solution and calculated by using the following equation (1) to obtain the FFA content (%) [16]. The FFA content of WCO in this work was 1.4%.

$$\text{FFA (\%)} = \frac{\text{(NaOH volume(mL)xNaOH normality (N) x fatty acid molecular weight)}}{\text{weight of sample (g)}} \text{x100} \quad (1)$$

The esterification of WCO was performed three times for each experiment in a 250-mL two-necked round-bottom reactor. The reactor was equipped with a reflux condenser, a thermocouple, and a heating mantle, and it was magnetically agitated. The chiller was equipped with a reflux condenser to re-condense the evaporated methanol in the reaction system, compensating for the methanol loss during the reaction. The reactor was fed with 33.9 g of WCO mixed with methanol. The mixture temperature was set at 60 °C using a heating mantle and stirred at 300 rpm. After the reaction, the catalyst was separated by filtration, and the liquid mixture was allowed to settle into two phases. The bottom layer, consisting of fatty acid methyl ester (FAME), was collected. The FAME layer was rinsed with hot distilled water several times [16]. The FAME product was also tested using paper chromatography. The FFA conversion (%) was calculated using the following equation (2), and the biodiesel mass yield (%) was calculated using equation (3). The effect of catalyst loading, reaction time, methanol to oil molar ratio, and temperature on the esterification reaction were investigated to determine the optimum condition in this work. Each experiment was conducted at least three times.

$$\text{FFA conversion (\%)} = \frac{\text{FFA of WCO (\%)-FFA of Biodiesel (\%)}}{\text{FFA of WCO (\%)}} \text{x100} \quad (2)$$

Where FFA of WCO (%) and FFA of Biodiesel (%) are FFA (%) of WCO and biodiesel calculated by equation (1), respectively.

$$\text{Biodiesel mass yield (\%)} = \frac{\text{Weight of biodiesel}}{\text{Weight of WCO}} \text{x100} \quad (3)$$

WCO (g) weight was measured before the reaction, while biodiesel (g) was measured after biodiesel purification.

Some physicochemical properties of the biodiesel produced, such as density using a pycnometer, viscosity using an Ostwald viscometer, acid value by titration, and iodine value by titration, were determined using the methods shown in Table 1.

Table 1. Selected requirements from Thailand, including the standard properties of biodiesel since 2019 and analytical methods.

Requirements		Standard range	Method
Density at 15 °C	kg/cm^3	860-900	ASTM D 1298
Viscosity at 40 °C	cSt	3.5-5.0	ASTM D 445
Acid value	mg_{KOH}/g	<0.5	ASTM D 664
Iodine value	g I_2/100 g	<120	ASTM D 6751

2.5 Reusability of the sulfonated CaO catalyst

The used catalyst from the optimum condition was collected, washed with n-hexane and methanol, and dried at 75 °C for 12 h before being used for the following reaction cycle at 5 wt% catalyst loading, a 9:1 methanol to oil ratio, a temperature of 65 °C, and a reaction time of 3 hours. FTIR and SEM then characterized the used catalyst.

3. Results and Discussion

3.1 Catalysts characterization

3.1.1 Investigation of functional groups on the surface of sulfonated/sulfated CaO catalysts

The spectra of bare CaO, 2 M sulfonated CaO, and 7 M sulfated CaO are shown in Figure 1. An FTIR peak in the wavenumber range of 3400–3600 cm^{-1} of spectrum (a) indicates stretching vibrations of the O-H bond with a sharp peak of -OH on bare CaO, which is caused by moisture bound to surface CaO [14]. After the sulfonation/sulfation process, the FTIR spectra of both samples are similar to those of hydrous calcium sulfate [17]. The sulfate functional groups can generally form strong Lewis acid sites and Brønsted acid sites when adsorbed on the metal oxide surface [13]. The sulfonated CaO catalyst has a Lewis acid site that accepts electrons. It can create a Brønsted acid site on the surface of the sulfonated CaO catalyst when it absorbs moisture representing -OH bonds and FTIR peaks appearing in the 3500-3600 cm^{-1} [13]. After the sulfation/sulfonation process, as shown in spectra (b) and (c), the sulfonated/sulfated CaO catalysts absorb less moisture. The FTIR band in 3400–3600 cm^{-1} becomes broader shifts to lower wavenumber, and two absorption bands at 3608 and 3554 cm^{-1} are observed, representing surface hydrogen bonding between surface moisture and sulfonic groups [18]. The intensity of these peaks decreases with increasing H_2SO_4 concentration from 2 M to 7 M, indicating lower hydrogen bonding in the 7 M treated CaO sample. A low-intensity FTIR peak at wavenumber 3695 cm^{-1} is observed on 2 M sulfonated CaO, representing the bonds between calcium ions and the OH groups [19]. The 2 M sulfonated CaO also shows a small peak at 3400 cm^{-1} corresponding to the –OH stretching of physically absorbed water molecules [15], but it is not observed on 7 M sulfated CaO. The new peaks in the 1400-1000 cm^{-1} region confirm the surface species of sulfate or sulfonate on CaO after the sulfation/sulfonation process [19]. Before the CaO sulfation/sulfonation process, FTIR peaks at 1413 and 875 cm^{-1} were observed, showing asymmetric stretching vibrations and out-of-plane bending vibrations of carbonate (CO_3^{2-}) caused by the absorption of CO_2 on CaO [20]. These vibrations were still observed with lower intensity for 2 M sulfonated CaO, indicating that CaO is still available on the surface after sulfonation but not observed for 7 M sulfated CaO. The FTIR signal at 1620 cm^{-1} represents the bending vibration bond of the hydroxyl (-OH) group connected to the sulfate (SO_4^{2-}) group, which could indicate the Brønsted acid site for the esterification. The vibration at around 1240 cm^{-1}, associated with the asymmetric vibration of S=O in bidentate SO_4^{2-} ions, was not observed for both 2 M and 7 M treated CaO [15]. A strong peak at wavenumber 1151 cm^{-1} shows asymmetric stretching vibrations of O=S=O and S-O bonds in $-SO_3H$ [12, 14, 15]. The wavenumber at 1093 cm^{-1} indicates symmetric stretching of O=S=O in $–SO_3^-$ [12, 15, 18, 20, 22-24]. However, the vibration splitting in this sulfate region is observed only for 2 M treated CaO. A small peak at wavenumber 1009 cm^{-1} also indicates other modes of S=O stretching of surface sulfate species on treated CaO [25]. The vibration splitting in this sulfate region indicates symmetrical changes or different modes of surface sulfate or

sulfonate species, such as free sulfate, monodentate, chelate bidentate, and bridge bidentate on metal oxides [19, 26]. The FTIR spectrum of 7 M treated CaO shows non-vibrational splitting, similar to that of sulfated CAWS-(7)SO_4 synthesized by Syazwani and co-workers [13]. The FTIR peak at wavenumber 673 cm^{-1} indicates S-O bending mode [23], and 603 cm^{-1} indicates Ca-O bonds [27]. Thus, the FTIR bands at 1151 and 1093 cm^{-1} suggest that CaO after reaction with 2 M H_2SO_4 is sulfonated CaO, while CaO after reaction with 7 M H_2SO_4 is sulfated CaO.

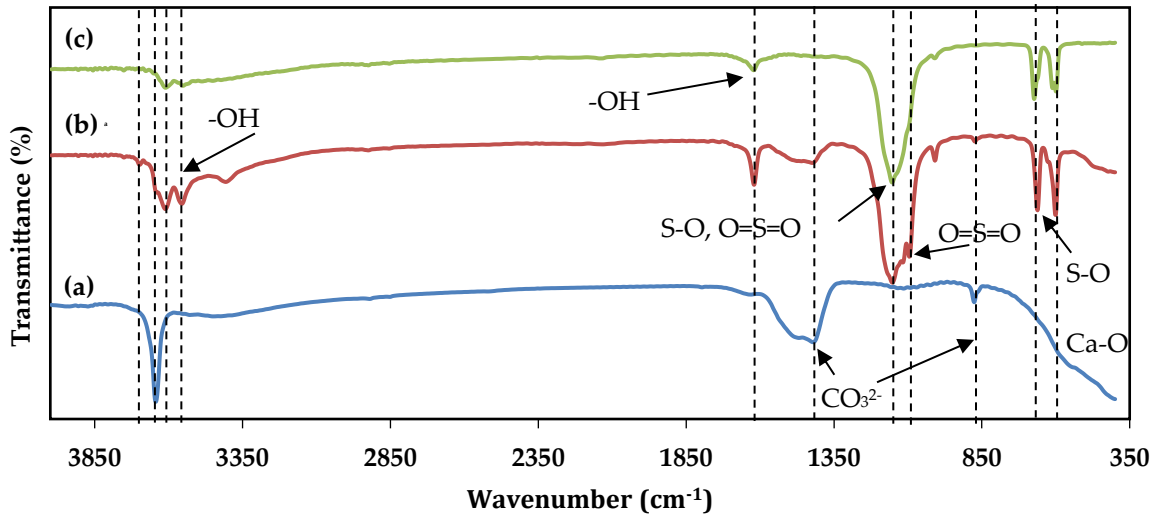

Figure 1. FTIR spectra of a) bare CaO, b) 2 M sulfonated CaO, c) 7 M sulfated CaO.

3.1.2 Morphological analysis of sulfonated/sulfated CaO catalysts

The morphology of bare CaO and synthesized sulfonated/sulfated CaO was investigated by SEM, as shown in Figure 2. Figure 2a reveals that bare CaO has a cubic crystal structure, and sulfonated CaO shows a rod-like structure. In contrast, sulfated CaO shows a hexagonal crystal structure, as shown in Figures 2b and 2c, indicating that the morphology of CaO changes as it is affected by the sulfuric acid concentration in the sulfation process. These SEM images show a change in the crystal structure after sulfonation/sulfation, which is consistent with the XRD results. It is shown that the crystal size increases with increasing sulfuric acid concentration. When compared with the work of [28], it is found that the concentration of 2 M causes a change in pores formed after the sulfonation reaction. As the acid concentration increased, the damage to the catalyst surface increased.

The surface element distribution characteristics of the sulfonated/sulfated CaO catalysts were determined by SEM-EDX, as shown in Figures 3 and 4, showing O, Ca, and S atoms on their surface. The 2 M sulfonated CaO catalyst had an O element equal to 48.9 %, which had a higher O atom content than the 7 M sulfated CaO catalyst, which is 46.4%, consistent with the results of FTIR and TPD, indicating that there was a functional group of M-OH and a stronger acidic strength on the catalyst than the 7 M sulfated CaO catalyst. When the concentration of sulfuric acid increases, the amount of S atom distribution increases accordingly, resulting in a reduction in the pore volume of the catalyst. This is consistent with the results of BET surface area in Table 4 [29].

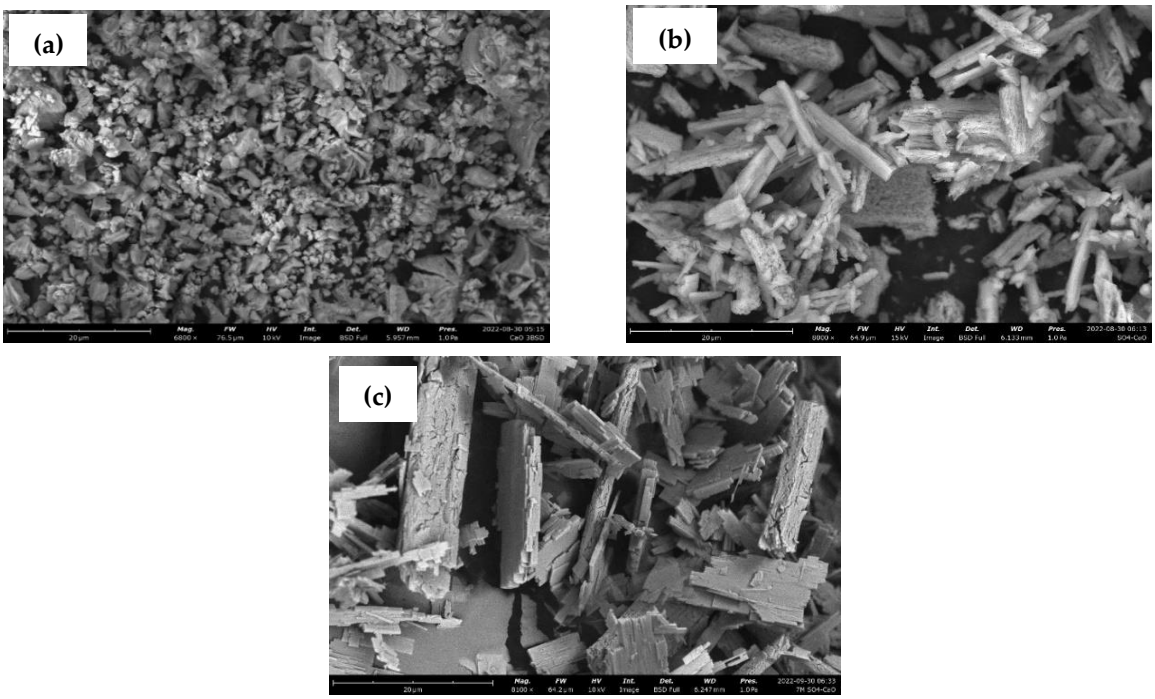

Figure 2. SEM images of a) bare CaO, b) 2 M sulfonated CaO, and c) 7 M sulfated CaO.

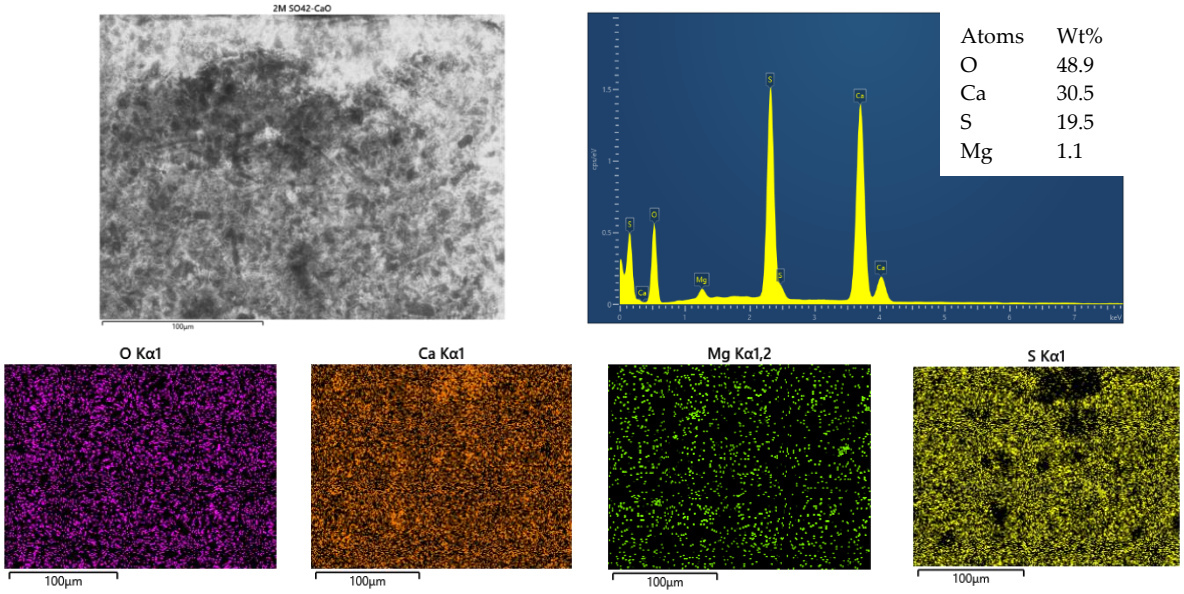

Figure 3. SEM-EDX image of 2 M sulfonated CaO catalyst.

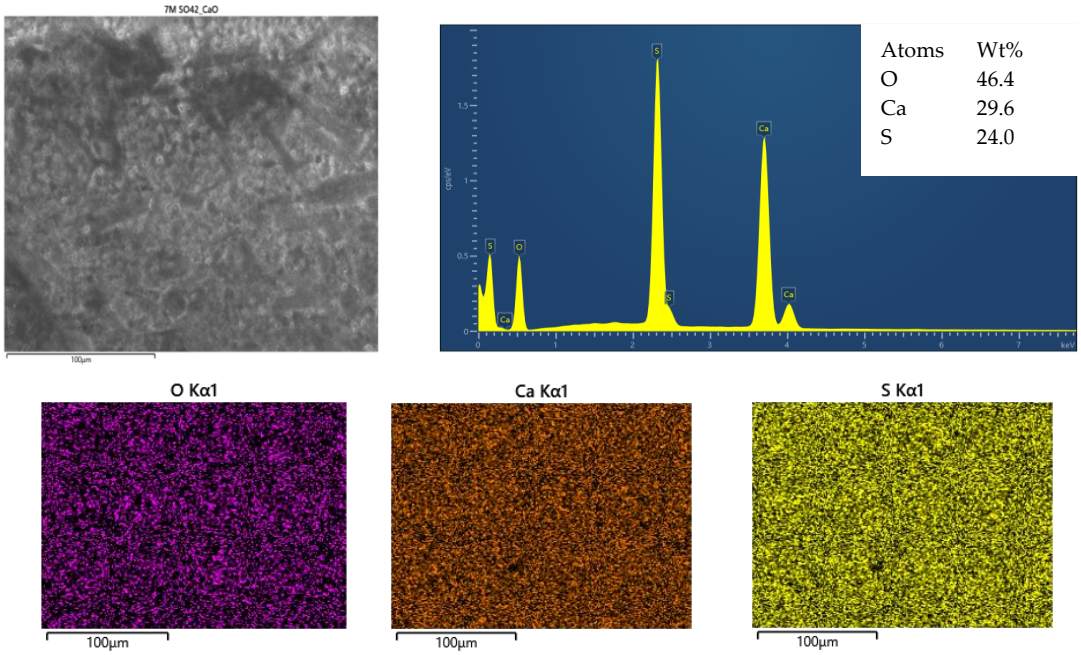

Figure 4. SEM-EDX image of 7 M sulfated CaO catalyst.

3.1.3 Crystal structure analysis of sulfonated/sulfated CaO catalysts

The phase and crystallinity of the 2 M sulfonated and 7 M sulfated CaO catalysts were determined, as shown in Figures 5a and 5b, respectively. The phase of $CaSO_4.2H_2O$ (JCPDS File: 21-0816) was observed. Figure 5a of the 2 M sulfonated CaO catalyst shows an XRD pattern at the 2θ position: 11.65, 20.76, 23.40, 31.12, 40.62, and 42.63, representing crystal planes at (020), (021), (040), (-221), (151), and (042) that have a monoclinic structure. The 7 M sulfated CaO catalyst showed XRD peaks at the 2θ position equal to 14.77, 25.72, 29.75, 31.84, and 49.32, which were similar to the hexagonal crystal form of $CaSO_4{\cdot}0.5H_2O$ (JCPDS File: 14-0224) [28], with follow crystal planes at (200), (020), (400), (204), and (424), respectively [30]. These XRD data demonstrated that the lattice anions of CaO had been replaced by sulfate ions, resulting in a new crystal structure of calcium sulfate.

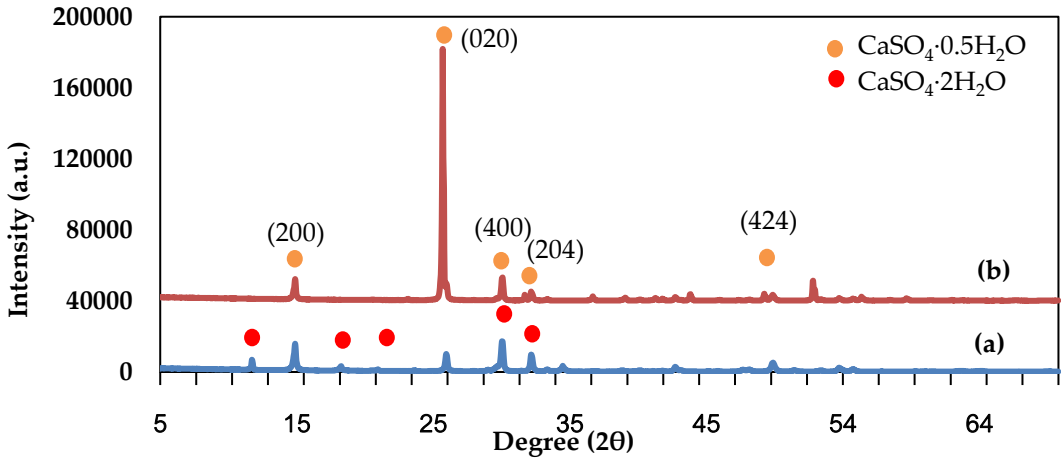

Figure 5. XRD patterns of (a) 2 M sulfonated CaO and (b) 7 M sulfated CaO catalysts.

3.1.3 Acidity-basicity analysis of sulfonated/sulfated CaO catalysts

The acidity-basicity of the sulfonated/sulfated CaO catalysts was investigated by TPD, as shown in Tables 2 and 3. By increasing the sulfuric acid concentration from 2 M to 7 M, the acid content of sulfonated CaO decreased from 7.22 to 0.05 mmol/g due to the structural change of CaO to $CaSO_4$. The NH_3-TPD profile (data not shown here) shows a desorption peak of NH_3 gas from the sulfonated CaO catalyst at a temperature of 200 °C, which indicates the presence of a weak acid site [14], while a peak position at 450–600 °C indicates the presence of a strong Lewis acid site. The data in Table 2 also shows that the 2 M sulfonated CaO catalyst had a higher acidity than the 7 M sulfated CaO catalyst. This acid content is also higher than that of the CAWS-$_{(7)}$ SO_4 catalyst (acid content of 4.73 mmol/g) prepared by Syazwani and co-workers [13] by burning angel wing shells and soaking them in 7 M sulfuric acid. It indicates that the 2 M sulfonated CaO catalyst may have more suitable catalytic properties than the 7 M sulfated CaO catalyst, which is consistent with the FTIR results indicating the -SO_3H group on the 2 M sulfonated CaO catalyst surface at 1151 cm^{-1}. This group acts as the activation and adsorption sites during the NH_3-TPD and catalytic processes. In addition, the basicity amounts of 2 M sulfonated CaO and 7 M sulfated CaO were 3.86 and 0.05 mmol/g, respectively, due to the adsorption of CO_2 on the residual Ca-O-Ca sites on the catalyst surface. [13, 31].

Table 2. NH_3-TPD and acidity data of sulfonated/sulfated CaO catalysts.

Catalysts	Temperature (°C)	Amount of NH_3 desorbed (mmol/g)	Total amount of acidity (mmol/g)
2 M sulfonated CaO	478.6	5.16	7.22
	741.2	2.06	
7 M sulfated CaO	93.2	0.02	0.05
	699.0	0.02	

Table 3. CO_2-TPD and basicity data of sulfonated/sulfated CaO catalysts.

Catalysts	Temperature (°C)	Amount of CO_2 desorbed (mmol/g)	Total amount of basicity (mmol/g)
2 M sulfonated CaO	97.1	0.05	3.86
	468.9	2.29	
	741.7	1.52	
7 M sulfated CaO	99.8	0.02	0.05
	680.6	0.03	

3.1.5 BET surface area investigation of sulfonated/sulfonated CaO catalysts.

The BET surface areas of the 2 M sulfonated and 7 M sulfated CaO catalysts were investigated, as shown in Table 4. Normally, the surface area of commercial CaO is equal to 3.98 m^2/g [28]. In this work, after chemical treatment with 2 and 7 M sulfuric acid, the surface area of the catalyst increased to 9.10 m^2/g and decreased to 3.51 m^2/g, respectively. This is because sulfonate ions from sulfuric acid are attached to the surface of CaO. When sulfuric acid concentration increases, the sulfate ions from the acid get stuck in CaO pores, decreasing the pore volume of the sulfated catalyst. This result is consistent with the SEM-EDX data in Figure 3, indicating an increase in the surface area of the 2 M sulfonated catalyst due to the sulfuric acid effect. Increasing surface area can increase reaction space and rate [20]. The nitrogen gas absorption and desorption profiles of the 2 M sulfonated and 7 M sulfated CaO catalysts are shown in Figure 5. The N_2-absorption and desorption of these catalysts represent a type IV adsorption isotherm, consisting of the multilayer adsorption of the gas sample with the mesopore size of the catalyst. The relative pressure region in the range of 0.0 to 0.1 shows monolayer adsorption; when the relative pressure increases, the adsorption still occurs, forming multilayers; then there is capillary condensation at a relative pressure range of 0.8 to 1, indicating a type 3 hysteresis loop [32]. In contrast to the CaO synthesized by [33] through calcination at 850 °C for 4 hours, the average pore diameter of the 2 M sulfonated CaO catalyst was 196.14 Å, which was greater than that of [33] (17.047 Å). Additionally, the pore volume was 0.045 cm^3/g, which was higher than the 0.036 cm^3/g synthesized

by [33] due to the reaction with sulfuric acid. The higher average pore diameter is possibly suitable for oil reactant mass transfer into the pore during catalysis.

Table 4. Surface properties of 2 M sulfonated and 7 M sulfated calcium oxide catalysts

Catalyst	BET surface area (m^2/g)	Average pore diameter (Å)	Pore volume (cm^3/g)
2 M sulfonated CaO	9.20	196.14	0.05
7 M sulfated CaO	3.51	190.32	0.02
CaO commercial [28]	3.98	3.82	0.02

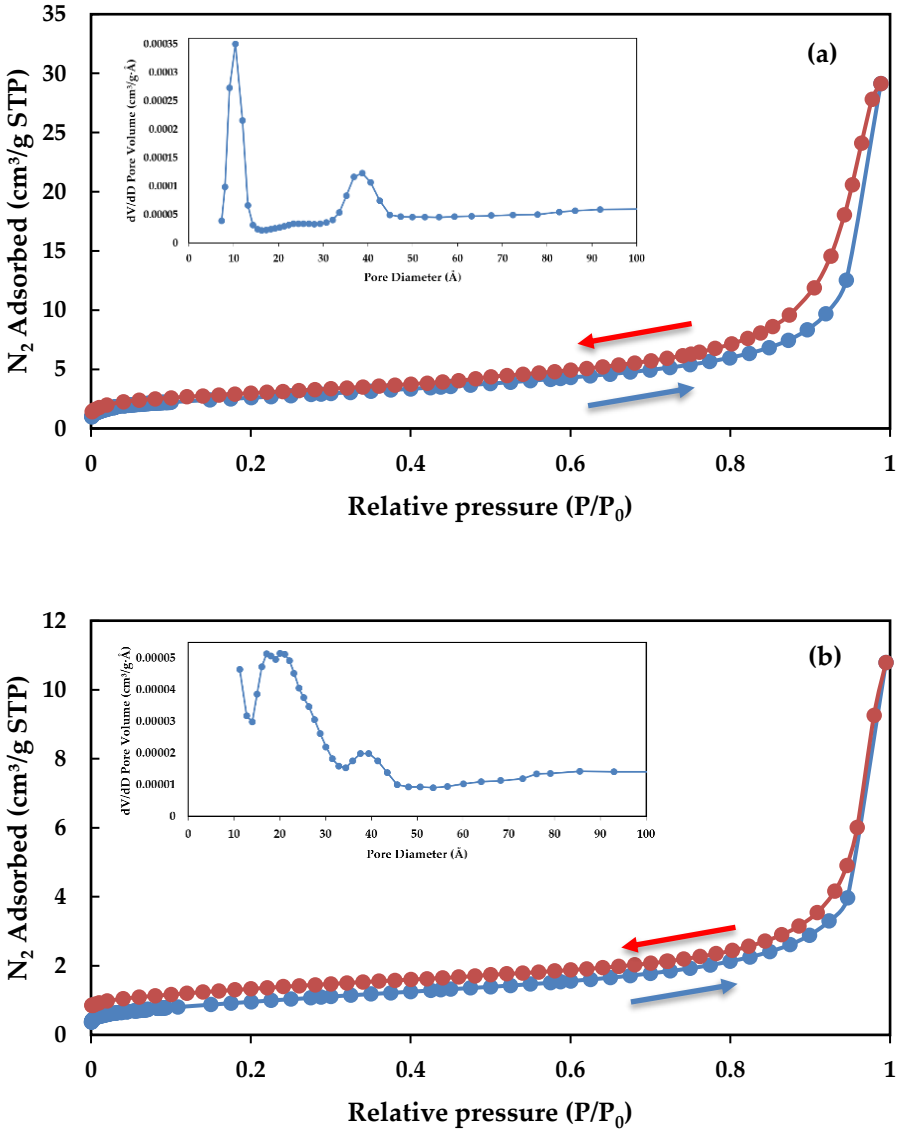

Figure 5. N_2-adsorption and desorption isotherms of (a) 2 M sulfonated calcium oxide and (b) 7 M sulfated calcium oxide catalysts with pore size distribution.

The inset in Figure 5 shows the pore size distribution of the sulfonated/sulfated CaO catalysts. It could be observed that upon chemical treatment of CaO with sulfuric acid, the CaO catalyst particles exhibited a pore size distribution that consisted of a primary pore at 10.41 Å and a secondary pore at 38.72 Å for 2 M sulfonated CaO, and a pore size distribution of 17.10, 21.06, and 39.46 Å for 7 M sulfated CaO. These pores can

be classified as mesopores [34]. Based on the characterization data, the 2 M sulfonated CaO catalyst was selected to catalyze esterification to produce biodiesel from WCO.

3.2 Optimization of biodiesel production

3.2.1 Effect of catalyst loading

The 2 M sulfonated CaO catalyst with various catalyst loadings of 3–9 wt%, a methanol to oil ratio of 9:1, and a reaction time of 3 h was selected to perform the esterification reaction at 65 °C. The biodiesel mass yield (%) and FFA conversion (%) are shown in Figure 6. It was found that the amount of catalysts in this work significantly affects the percentage of FFA conversion but is not significant for biodiesel mass yield (%). At the amount of catalyst equal to 5 wt%, the biodiesel mass yield is 61.19%, with the highest FFA conversion, 69.65%. The reaction may primarily be esterification; fatty acid interacts first at the Brønsted acid site of Ca-SO_3H, then methanol attacks to form an intermediate, thereby continuing the reaction [15]. However, when the amount of catalyst is greater than 5 wt%, FFA conversion slightly decreases due to a high amount of catalyst that affects the mixture's viscosity during mixing, resulting in poor interaction between oil and the catalyst. In addition, excess catalysts can adsorb the product on the catalyst's surface [35]. The 2 M sulfonated CaO catalyst in this work at 5 wt% catalyst gave a similar percentage when compared with the $SO_4^{2-}/Fe_3O_4–Al_2O_3$ catalyst at a catalyst dosage of 8 wt% for biodiesel production, showing FFA conversion was 66.8% [36]. Therefore, a catalyst amount of 5 wt% was selected to find the best condition.

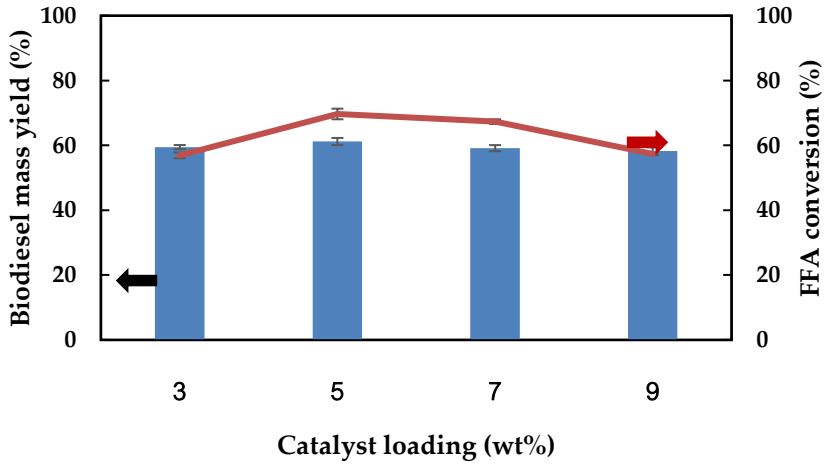

Figure 6. Effect of catalyst amount on biodiesel mass yield (%) and FFA conversion (%) using a methanol to oil ratio of 9:1, a temperature of 65 °C, and a reaction time of 3 h.

3.2.2 Effect of methanol to oil molar ratio

The effect of the methanol to oil ratio between 6:1, 9:1, and 15:1 using a 2 M sulfonated CaO catalyst at 5 wt%, a reaction time of 3 h, and a temperature of 65 °C were performed for the esterification reaction. The amount of methanol makes the reaction proceed forward to produce FAME. From Figure 7, the biodiesel mass yield is 66.77%, and the highest FFA conversion occurs at the methanol to oil ratio of 9:1. The FFA conversion obtained was 72.16%. When the methanol to oil ratio increased to 15:1, the mass yield and FFA conversion decreased to 65.65 and 67.64%, respectively. This data is consistent with data from the work of [31]; at the conditions of catalyst loading of 3.5 wt%, temperature of 150 °C, reaction time equal to 6 h, and methanol to oil molar ratio of 12:1, the amount of FFA conversion was equal to 83.26%. When the ratio of methanol to oil increases above 12:1, the FFA conversion (%) decreases as well due to two reasons: (1) the dissolution of glycerol in methanol inhibits the reaction with the reactant, and (2) excess methanol may reduce the active site of the catalyst and cause deactivation [36].

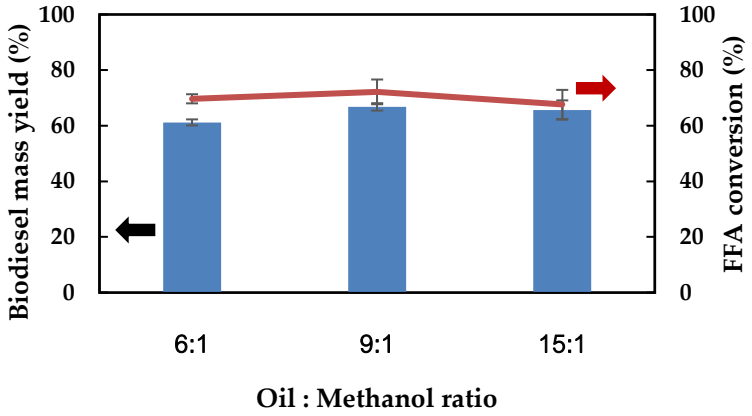

Figure 7. Effect of methanol to oil molar ratio on biodiesel mass yield (%) and FFA conversion (%) using 2 M sulfonated CaO, catalyst loading 5 wt%, temperature 65 °C, reaction time 3 h.

3.2.3 Effect of temperature

The 2 M sulfonated CaO catalyst with 5 wt% catalyst loading, a methanol: oil ratio of 9:1, and a reaction time of 3 hours was selected to perform the effect of esterification temperature, as shown in Figure 8. When the temperature increased from 55 to 70 °C, a mass yield of 68.93% and the highest FFA conversion of 84.93% were observed at a temperature of 65 °C, which is consistent with the work of Jamil and co-workers [37] at the temperature of 65 °C, with the highest biodiesel content being 94.27%. Normally, high temperatures used in the reaction increase the rate of the esterification reaction. The viscosities of methanol and oil decrease with high reaction temperatures, causing more homogeneity [38]. The effect of temperature on the reaction rate can be explained through the kinetic theory of chemical reactions. An increase in temperature results in higher molecular speeds and an increased reaction rate [39]. However, the reaction at temperatures higher than 70 °C was not possible in this work due to the limitations of the apparatus and the reflux temperature of methanol under normal pressure [40]. Thus, the FFA conversion in this work decreased from 84.93 to 37.89% when the temperature increased. The methanol used in the reaction evaporates and cannot be condensed to react with the oil [41].

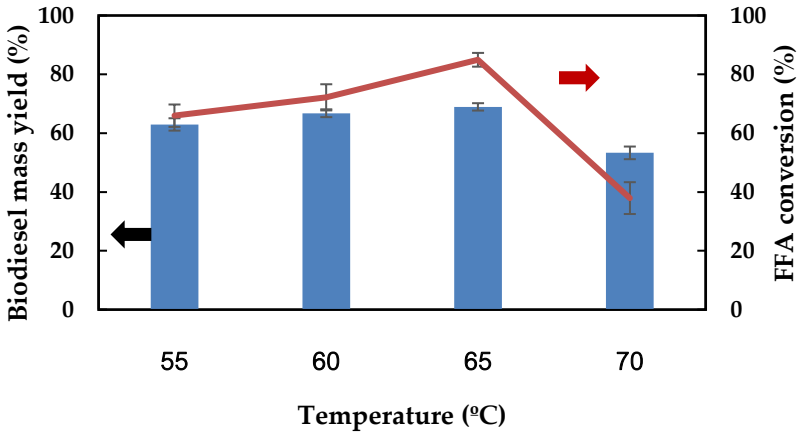

Figure 8. Effect of temperature on FFA conversion using 2 M sulfonated CaO at 5 wt%, methanol to oil molar ratio was 9:1, and reaction time of 3 h.

3.2.4 Effect of reaction time

The effect of reaction time at 3, 6, and 9 hours for esterification of WCO was investigated using the 2 M sulfonated CaO catalyst with 5 wt% catalyst loading, a methanol: oil ratio of 9:1, and a temperature of 65 °C. The result is shown in Figure 9. At 3 hours, the mass yield was 66.96%, and the FFA conversion was 84.93%.

When the reaction time increases by 6 and 9 hours, the FFA conversion decreases to 77.17 and 71.97%, respectively. The decrease in FFA conversion is consistent with the work of [42], with the highest biodiesel amount equaling 94.6% at reaction time 3. h. After 3 hours, FFA conversion gradually decreased to a similar level. At first, the biodiesel reaction may be low due to the reactants' low compatibility. Then, as the duration increases, compatibility increases. However, if the reaction time exceeds 3 hours, the higher product concentration gradually reduces the biodiesel yield, leading to a quick reaction reverse [43]. The best reaction time when using a homogeneous catalyst is generally 30–120 minutes [44], while the best reaction time for heterogeneous catalysts is 180 minutes or 3 hours [45]. The 2 M sulfonated CaO catalyst used in this work was also optimized at 3 hours, and the best condition was that the catalyst amount was 5 wt%, the methanol: oil ratio was 9:1, and the temperature was 65 °C. Table 5 shows that the acid value of the biodiesel product is 0.18 mg KOH/g of the sample, which is lower than the maximum limit of Thailand's standard biodiesel. Furthermore, the viscosity at 40 °C and density at 15 °C of the biodiesel product in this work fall in the standard range. According to Giakoumis and co-workers [46], the viscosity of the produced fuel influences its fluidity and atomization; a higher viscosity could result in poor atomization and less accurate fuel injector operation.

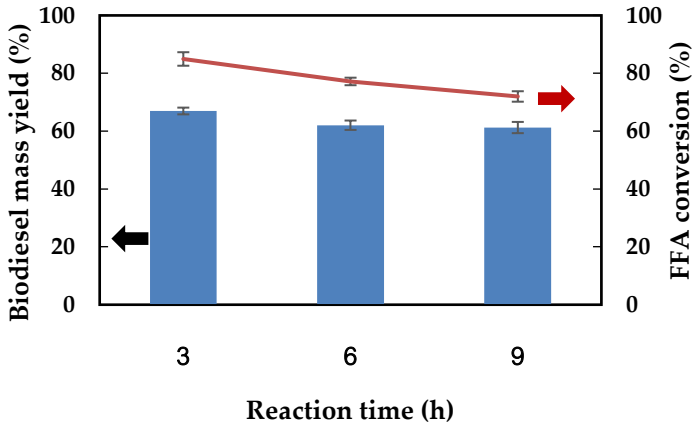

Figure 9. Effect of reaction time on FFA conversion using 2 M sulfonated CaO at 5 wt%, methanol to oil ratio of 9:1, and a temperature of 65 °C.

Table 5. Characteristics and important qualities of biodiesel product using catalyst content of 5 wt%, methanol: oil ratio of 9:1, temperature of 65 ºC, and 3 h reaction times.

Requirements		Thailand standard range	WCO	biodiesel
Density at 15 °C	kg/cm^3	860-900	949.67 ± 3.86	873.43 ± 19.81
Viscosity at 40 °C	cSt	3.5-5.0	14.81 ± 1.34	4.36 ± 0.60
Acid value	mg$_{KOH}$/g	<0.5	1.4 ± 0.24	0.18 ± 0.05
Iodine value	g I_2/100 g	<120	88.22 ± 1.29	27.42 ± 3.44

3.2.5 Reusability of sulfonated CaO catalyst

Ideal catalysts can be reused many times before deactivation takes place. In this work, the catalyst obtained from the optimum condition was washed with n-hexane and methanol and then dried at 70 °C for 12 hours before the next esterification reaction. The reusability data is shown in Figure 10. The percentage of FFA conversion gradually decreased with the reuse of the catalyst in the 3rd round and significantly decreased in the 4th and 5th rounds. The decrease in FFA conversion may be due to the deactivation of the catalyst, causing coke or chemical residues at the active sites with unreacted oil and glycerol [47], which is consistent with the SEM image in Figure 11, indicating a change in the size of the catalyst to larger sizes than a fresh catalyst, which affects the surface area of the catalyst. Thus, the surface area of the catalyst reduces after the catalysis of esterification. In addition, glycerol may remain adsorbed on the surface of the catalyst. This is consistent with the FTIR results as shown in Figure 12, with peaks appearing at wavenumber 2919 and 1467 cm^{-1},

representing the vibrational of the C-H bond stretching for alkane and O-CH_2 groups, respectively, which may be glycerol and mono, di, and triglycerides remaining on the surface of the catalyst. However, an FTIR peak at 1151 cm^{-1} is still observed, which is an asymmetric stretching vibration of the O=S=O of sulfonate groups [12, 14, 15] and 1093 cm^{-1} represents the symmetric stretching of O=S=O in -SO_3^- [12, 15, 18, 20, 22-24]. The ions do not easily escape during biodiesel production due to the strong bond between the calcium group's positive charge and the sulfonate group negative charge [15, 20].

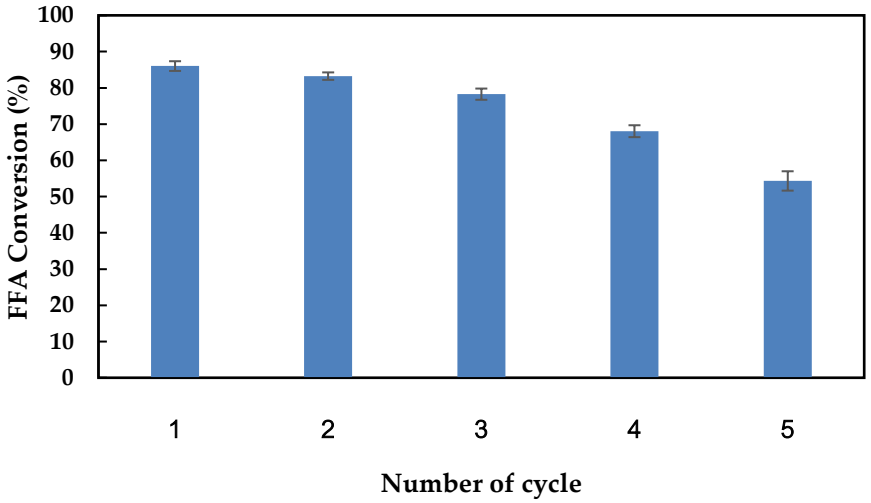

Figure 10. Effect of reuse of a 2 M sulfonated CaO catalyst at 5 wt%, methanol to oil ratio of 9:1, the temperature of 65 °C, and 3 h reaction time.

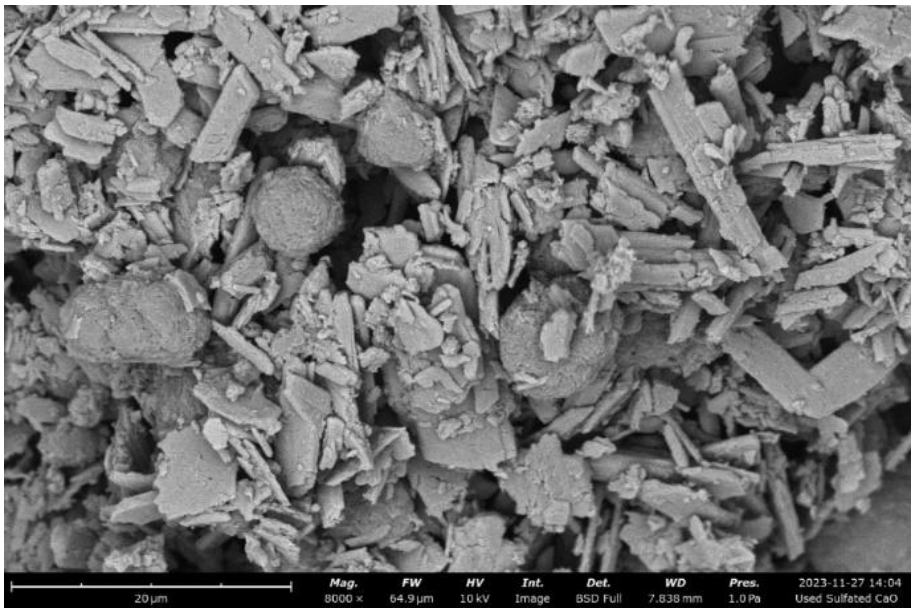

Figure 11. SEM images of reuse 2 M sulfonated CaO.

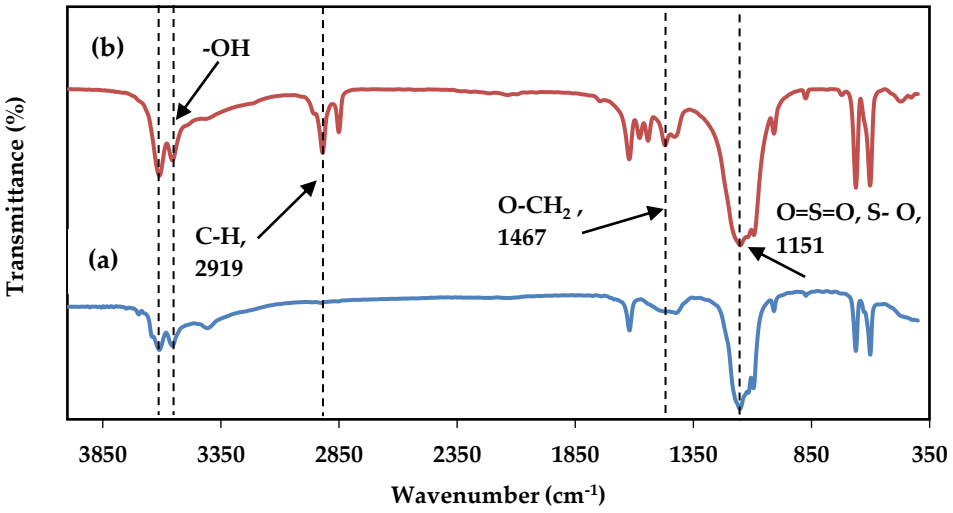

Figure 12. FTIR spectra of (a) fresh 2 M sulfonated CaO and (b) used 2 M sulfonated CaO catalyst.

3.2.6. Proposed mechanism of esterification catalyzed by sulfonated CaO catalyst

The reaction mechanism for the esterification of WCO by the 2 M sulfonated CaO catalyst to produce biodiesel is proposed in Figure 13 based on FTIR and TPD data. When the electrophilic carbonyl group or carboxylic acid group (-COOH) in the FFA molecule reacts with a proton (H^+) at the Brønsted acid sites ($-SO_3H$), a carbocation is formed on the surface of the catalyst. Then, the methanol molecule attacks the carbocation to form an intermediate. A proton shifts from the oxonium ion to the -OH group, forming an activated complex. These intermediates proceed to eliminate a water molecule, resulting in a protonated alkyl ester. The desorption of the alkyl ester from the Brønsted acid site (deprotonation) restores the catalyst [15, 48]. Lewis acid sites (metal ions in low coordination) can also catalyze esterification, as proposed in Figure 14. The presence of Ca active sites in the catalyst can cause strong bonds with the carbonyl oxygen to form intermediate complexes, followed by interactions between the oxygen atoms of methanol and carbonyl carbon. The next step involves the loss and gain of a proton at one oxygen atom to form another intermediate, which in turn loses a water molecule and yields a protonated ester [48]. However, the adsorption of FFA molecules at Lewis acid sites may occur less than at Brønsted acid sites due to the large size of the FFA.

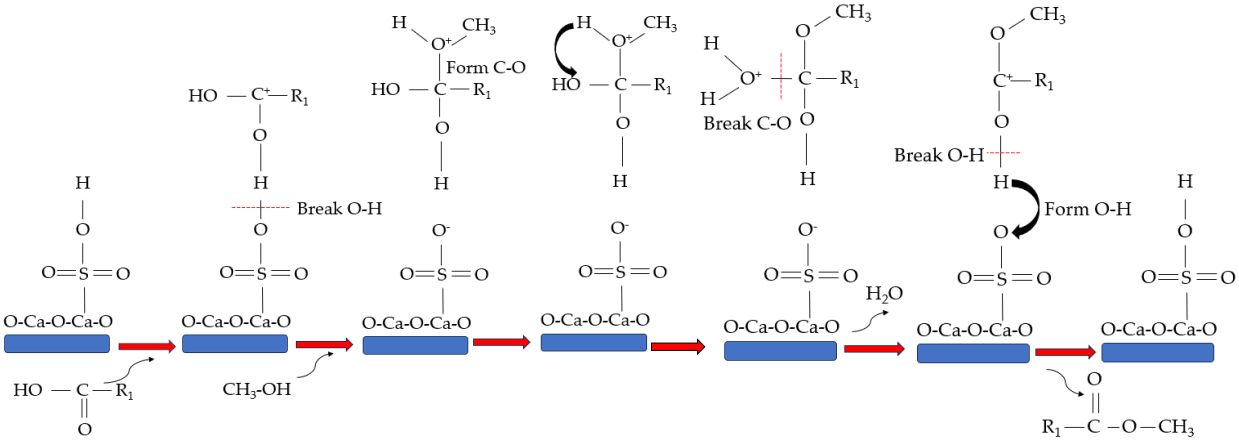

Figure 13. Propose mechanism of esterification using 2 M sulfonated CaO catalyst through Brønsted acid site.

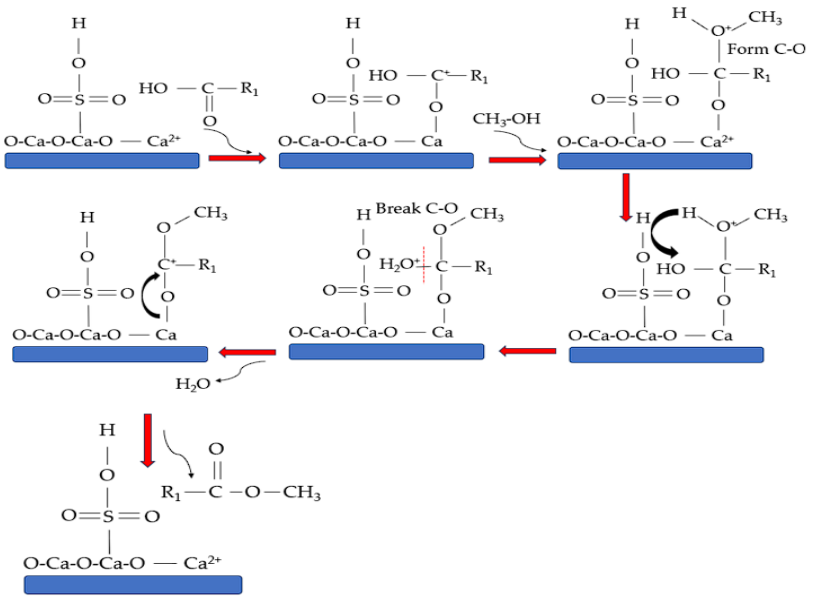

Figure 14. Propose esterification mechanism using 2 M sulfonated CaO catalyst through Lewis acid sites.

4. Conclusions

Sulfonation CaO successfully prepared the low-cost sulfonated CaO catalyst in sulfuric acid at a concentration of 2 M. The surface area increased from 3.98 to 9.20 m^2/g due to this process. The 2 M sulfonated CaO catalyst was found to have an acidity of 7.22 mmol/g and a basicity of 3.86 mmol/g. The optimum conditions for the esterification of WCO to produce biodiesel were determined by utilizing a 2 M sulfonated CaO catalyst, a methanol to oil ratio of 9:1, a reaction time of 3 hours, and a catalyst quantity of 5 wt%. The reaction was conducted at a temperature of 65 ˚C. The efficiency of FFA conversion was 84.9% in the reaction catalyzed by a 2 M sulfonated CaO catalyst. Additionally, the catalyst can be reused at least 2 times by washing it with n-hexane and methanol, provided that optimal conditions are maintained. This cost-effective sulfonated CaO catalyst exhibits promise for further exploration as an industrial catalyst in biodiesel production from edible and non-edible oils with a high free fatty acid, including waste cooking oil.

5. Acknowledgements

Author Contributions: Investigation, writing—original draft preparation: C.D.; conceptualization, methodology: R.J. and P.K.; writing-review and editing: T.C.; supervision, writing-review, and editing: S.C. All authors have read and agreed to the published version of the manuscript.

Funding: This research was financially supported by the Graduate School Dissertation Funding for Thesis, Prince of Songkla University, and Tuition Fee Grants for Graduate Students, Faculty of Science and Technology, Prince of Songkla University.

Conflicts of Interest: The authors declare no conflict of interest.

References

[1] Farabi, M. S. A.; Ibrahim, M. L.; Rashid, U.; Taufiq-Yap, Y. H. Esterification of palm fatty acid distillate using sulfonated carbon-based catalyst derived from palm kernel shell and bamboo. *Energy Conversion and Management* **2019**, *181*(September 2018), 562–570. https://doi.org/10.1016/j.enconman.2018.12.033

[2] Amenaghawon, A. N.; Obahiagbon, K.; Isesele, V.; Usman, F. Optimized biodiesel production from waste cooking oil using a functionalized bio-based heterogeneous catalyst. *Cleaner Engineering and Technology* 2022, *8*(April), 1-11. 100501. https://doi.org/10.1016/j.clet.2022.100501

[3] Baskar, G.; Kalavathy, G.; Aiswarya, R.; Abarnaebenezer Selvakumari, I. Advances in bio-oil extraction from nonedible oil seeds and algal biomass. *In Advances in Eco-Fuels for a Sustainable Environment* **2019**, 187–210. Elsevier. https://doi.org/10.1016/B978-0-08-102728-8.00007-3

[4] Okoduwa, I. G.; Oiwoh, O.; Amenaghawon, A. N.; Okieimen, C. O. A biobased mixed metal oxide catalyst for biodiesel production from waste cooking oil: reaction conditions modeling, optimization and sensitivity analysis study. *Journal of Engineering Research (Kuwait)* **2024**, February. https://doi.org/10.1016/j.jer.2024.03.009

[5] Deeba, F.; Kumar, B.; Arora, N.; Singh, S.; Kumar, A.; Han, S. S.; Negi, Y. S. Novel bio-based solid acid catalyst derived from waste yeast residue for biodiesel production. *Renewable Energy* **2020**, *159*, 127–139. https://doi.org/10.1016/j.renene.2020.05.029

[6] Chanakaewsomboon, I.; Tongurai, C.; Photaworn, S.; Kungsanant, S.; Nikhom, R. Investigation of saponification mechanisms in biodiesel production: Microscopic visualization of the effects of FFA, water and the amount of alkaline catalyst. *Journal of Environmental Chemical Engineering* **2020**, *8*(2), 1-40. https://doi.org/10.1016/j.jece.2019.103538

[7] Etim, A. O.; Musonge, P.; Eloka-Eboka, A. C. An effective green and renewable heterogeneous catalyst derived from the fusion of bi-component biowaste materials for the optimized transesterification of linseed oil methyl ester. *Biofuels, Bioproducts and Biorefining* **2021**, *15*(5), 1461–1472. https://doi.org/10.1002/bbb.2252

[8] Kedir, W. M.; Wondimu, K. T.; Weldegrum, G. S. Optimization and characterization of biodiesel from waste cooking oil using modified CaO catalyst derived from snail shell. *Heliyon* **2023**, *9*(5), e16475. https://doi.org/10.1016/j.heliyon.2023.e16475

[9] Faruque, M. O.; Razzak, S. A.; Hossain, M. M. Application of heterogeneous catalysts for biodiesel production from microalgal oil—a review. *Catalysts* **2020**, *10*(9), 1–25. https://doi.org/10.3390/catal10091025

[10] Al-Saadi, A.; Mathan, B.; He, Y. Biodiesel production via simultaneous transesterification and esterification reactions over SrO–ZnO/Al_2O_3 as a bifunctional catalyst using high acidic waste cooking oil. *Chemical Engineering Research and Design* **2020**, *162*(2018), 238–248. https://doi.org/10.1016/j.cherd.2020.08.018

[11] Chen, G. Y.; Shan, R.; Yan, B. B.; Shi, J. F.; Li, S. Y.; Liu, C. Y. Remarkably enhancing the biodiesel yield from palm oil upon abalone shell-derived CaO catalysts treated by ethanol. *Fuel Processing Technology*, **2016**, *143*, 110–117. https://doi.org/10.1016/j.fuproc.2015.11.017

[12] Istadi, I.; Anggoro, D. D.; Buchori, L.; Rahmawati, D. A.; Intaningrum, D. Active acid catalyst of sulphated zinc oxide for transesterification of soybean oil with methanol to biodiesel. *Procedia Environmental Sciences* **2015**, *23*, 385–393. https://doi.org/10.1016/j.proenv.2015.01.055

[13] Syazwani, O. N.; Rashid, U.; Mastuli, M. S.; Taufiq-Yap, Y. H. Esterification of palm fatty acid distillate (PFAD) to biodiesel using Bi-functional catalyst synthesized from waste angel wing shell (*Cyrtopleura costata*). *Renewable Energy* **2019**, *131*, 187–196. https://doi.org/10.1016/j.renene.2018.07.031

[14] Syazwani, O. N.; Ibrahim, M. L.; Wahyudiono, Kanda, H.; Goto, M.; Taufiq-Yap, Y. H. Esterification of high free fatty acids in supercritical methanol using sulfated angel wing shells as catalyst. *Journal of Supercritical Fluids* **2017**, *124*, 1–9. https://doi.org/10.1016/j.supflu.2017.01.002

[15] Valizadeh, S.; Valizadeh, B.; Khani, Y.; Jae, J.; Hyun Ko, C.; Park, Y. K. Production of biodiesel via esterification of coffee waste-derived bio-oil using sulfonated catalysts. *Bioresource Technology* **2024**, *404*(May), 130908. https://doi.org/10.1016/j.biortech.2024.130908

[16] Kouzu, M.; Kasuno, T.; Tajika, M.; Sugimoto, Y.; Yamanaka, S.; Hidaka, J. Calcium oxide as a solid base catalyst for transesterification of soybean oil and its application to biodiesel production. *Fuel* **2008**, 87(12), 2798–2806. https://doi.org/10.1016/j.fuel.2007.10.019

[17] Kiefer, J.; Strk, A.; Kiefer, A. L.; Glade, H. Infrared spectroscopic analysis of the inorganic deposits from water in domestic and technical heat exchangers. *Energies* **2018**, *11*(4). https://doi.org/10.3390/en11040798

[18] Juan-Alcañiz, J.; Gielisse, R.; Lago, A.B.; Ramos-Fernandez, E.V.; Serra-Crespo, P.; Devic, T.; Guillou, N. Serre, C.; Kapteijna, F.; Gascon; J. Towards acid MOFs-catalytic performance of sulfonic acid functionalized architectures. *Catalysis Science & Technology* **2013**, *3*(9), 2311–2318, https://doi: 10.1039/c3cy00272a

[19] Nayebzadeh, H.; Hojjat, M. Fabrication of SO_4^{2-}/MO–Al_2O_3–ZrO_2 (M = Ca, Mg, Sr, Ba) as solid acid–base nanocatalyst used in trans/esterification reaction. *Waste and Biomass Valorization*, **2020**, *11*(5), 2027–2037. https://doi.org/10.1007/s12649-018-0526-0

[20] Liu, F.; Ma, X.; Li, H.; Wang, Y.; Cui, P.; Guo, M.; Yaxin, H.; Lu, W.; Zhou, S.; Yu, M. Dilute sulfonic acid post functionalized metal organic framework as a heterogeneous acid catalyst for esterification to produce biodiesel. Fuel, **2020**, *266*(January), 117149. https://doi.org/10.1016/j.fuel.2020.117149

[21] Hussein, A. I.; Ab-Ghani, Z.; Mat, A. N. C.; Ghani, N. A. A.; Husein, A.; Rahman, I. A. Synthesis and characterization of spherical calcium carbonate nanoparticles derived from cockle shells. *Applied Sciences (Switzerland)* **2020**, *10*(20), 1–14. https://doi.org/10.3390/app10207170

[22] Farabi, M. S. A.; Ibrahim, M. L.; Rashid, U., Taufiq-Yap, Y. H. Esterification of palm fatty acid distillate using sulfonated carbon-based catalyst derived from palm kernel shell and bamboo. *Energy Conversion and Management* **2019**, *181*(September), 562–570. https://doi.org/10.1016/j.enconman.2018.12.033

[23] Xiong, X.; Yu, I. K. M.; Chen, S. S.; Tsang, D. C. W.; Cao, L.; Song, H.; Kwon, E. E.; Ok, Y. S.; Zhang, S.; Poon, C. S. Sulfonated biochar as acid catalyst for sugar hydrolysis and dehydration. *Catalysis Today* **2018**, *314*(February), 52–61. https://doi.org/10.1016/j.cattod.2018.02.034

[24] Melo H. P.; Cruz, A. J.; Candeias, A.; Mirão, J.; Cardoso, A. M.; Oliveira, M. J.; Valadas, S. Problems of analysis by FTIR of calcium sulphate-based preparatory layers: The case of a group of 16th-century Portuguese paintings. *Archaeometry* **2014**, *56*(3), 513–526. https://doi: 10.1111/arcm.12026

[25] Tangboriboon, N.; Unjan, W.; Sangwan, W.; Sirivat, A. Preparation of anhydrite from eggshell via pyrolysis. *Green Processing and Synthesis* **2018**, *7*(2), 139–146. https://doi.org/10.1515/gps-2016-0159

[26] McQuillan, A. J.; Osawa, M.; Peak, D.; Ren, B.; Tian, Z. Q. Experiments on adsorption at hydrous metal oxide surfaces using attenuated total reflection infrared spectroscopy (ATRIRS) (IUPAC Technical Report). *Pure and Applied Chemistry*, **2019**, *91*(12), 2043–2061. https://doi.org/10.1515/pac-2019-0211

[27] Ali, R. M.; Abd El Latif, M. M; Farag, H. A. Preparation and characterization of $CaSO_4$–SiO_2–CaO/SO_4^{2-} composite for biodiesel production. *American Journal of Applied Chemistry* **2015**, *3*(3-1), 38-45. https://doi: 10.11648/j.ajac.s.2015030301.16.

[28] Zhu, Z.; Liu, Y.; Cong, W.; Zhao, X.; Janaun, J.; Wei, T.; Fang, Z. Soybean biodiesel production using synergistic CaO/Ag nano catalyst: Process optimization, kinetic study, and economic evaluation. *Industrial Crops and Products* **2021**, *166*(666), 113479. https://doi.org/10.1016/j.indcrop.2021.113479

[29] Shi, G.; Yu, F.; Wang, Y.; Pan, D.; Wang, H.; Li, R. A novel one-pot synthesis of tetragonal sulfated zirconia catalyst with high activity for biodiesel production from the transesterification of soybean oil. *Renewable Energy* **2016**, *92*, 22–29. https://doi.org/10.1016/j.renene.2016.01.094

[30] Zhang, G.; Cao, D.; Wang, X.; Guo, S.; Yang, Z.; Cui, P.; Wang, Q.; Dou, Y.; Cheng, S.; Shen, H. α-calcium sulfate hemihydrate with a 3D hierarchical straw-sheaf morphology for use as a remove Pb^{2+} adsorbent. *Chemosphere* **2022**, *287*. https://doi.org/10.1016/j.chemosphere.2021.132025

[31] Marchetti, J. M.; Pedernera, M. N.; Schbib, N. S. Production of biodiesel from acid oil using sulfuric acid as catalyst: Kinetics study. *International Journal of Low-Carbon Technologies* **2011**, *6*(1), 38–43. https://doi.org/10.1093/ijlct/ctq040

[32] Ganesan, S.; Nadarajah, S.; Chee, X. Y.; Khairuddean, M.; Teh, G. B. Esterification of free fatty acids using ammonium ferric sulphate-calcium silicate as a heterogeneous catalyst. *Renewable Energy* **2020**, *153*, 1406–1417. https://doi.org/10.1016/j.renene.2020.02.094

[33] Sunarno, Zahrina, I.; Reni Yenti, S.; Sri Irianty, R.; Setia Utama, P. Catalytic co-pyrolysis of palm oil empty fruit bunch and waste tire using calcium oxide catalysts for upgrading bio-oil. *Materials Today: Proceedings* **2023**, *87*, 321–326. https://doi.org/10.1016/j.matpr.2023.03.290

[34] Lani, N. S.; Ngadi, N.; Yahya, N. Y.; Rahman, R. A. Synthesis, characterization and performance of silica impregnated calcium oxide as heterogeneous catalyst in biodiesel production. *Journal of Cleaner Production* **2017**, *146*, 116–124. https://doi.org/10.1016/j.jclepro.2016.06.058

[35] Farooq, M.; Ramli, A.; Subbarao, D. Biodiesel production from waste cooking oil using bifunctional heterogeneous solid catalysts. *Journal of Cleaner Production* **2013**, *59*, 131–140. https://doi.org/10.1016/j.jclepro.2013.06.015

[36] Safakish, E.; Nayebzadeh, H.; Saghatoleslami, N.; Kazemifard, S. Comprehensive assessment of the preparation conditions of a separable magnetic nanocatalyst for biodiesel production from algae. *Algal Research* **2020**, *49*(May), 101949. https://doi.org/10.1016/j.algal.2020.101949

[37] Jamil, F.; Murphin Kumar, P. S.; Al-Haj, L.; Tay Zar Myint, M.; Al-Muhtaseb, A. H. Heterogeneous carbon-based catalyst modified by alkaline earth metal oxides for biodiesel production: parametric and kinetic study. *Energy Conversion and Management: X* **2021**, *10*(May 2020), 100047. 1-10. https://doi.org/10.1016/j.ecmx.2020.100047

[38] Abdelhady, H. H.; Elazab, H. A.; Ewais, E. M.; Saber, M.; El-Deab, M. S. Efficient catalytic production of biodiesel using nano-sized sugar beet agro-industrial waste. *Fuel* **2020**, *261*(October 2019), 116481. 1-12. https://doi.org/10.1016/j.fuel.2019.116481

[39] Abbah, E. C.; Nwandikom, G. I.; Egwuonwu, C. C.; Nwakuba, N. R. Effect of reaction temperature on the yield of biodiesel from neem seed oil. *American Journal of Energy Science* **2016**, *3*(3), 16–20. http://www.openscienceonline.com/journal/energy

[40] Xie, W.; Wan, F. Basic ionic liquid functionalized magnetically responsive Fe_3O_4@HKUST-1 composites used for biodiesel production. *Fuel* **2018**, *220*(February), 248–256. https://doi.org/10.1016/j.fuel.2018.02.014

[41] Hazmi, B.; Rashid, U.; Ibrahim, M. L.; Nehdi, I. A.; Azam, M.; Al-Resayes, S. I. Synthesis and characterization of bifunctional magnetic nano-catalyst from rice husk for production of biodiesel. *Environmental Technology and Innovation* **2021**, 21, 101296. https://doi.org/10.1016/j.eti.2020.101296

[42] Mokhatr Mohamed, M.; El-Faramawy, H. An innovative nanocatalyst α-Fe_2O_3/AlOOH processed from gibbsite rubbish ore for efficient biodiesel production via utilizing cottonseed waste oil. *Fuel* **2021**, *297*(May 2020), 120741. https://doi.org/10.1016/j.fuel.2021.120741

[43] Xia, S.; Li, J.; Chen, G.; Tao, J.; Li, W.; Zhu, G. Magnetic reusable acid-base bifunctional Co Doped $Fe2O_3$–CaO nanocatalysts for biodiesel production from soybean oil and waste frying oil. *Renewable Energy* **2022**, *189*, 421–434. https://doi.org/10.1016/j.renene.2022.02.122

[44] Verma, P.; Sharma, M. P. Review of process parameters for biodiesel production from different feedstocks. *Renewable and Sustainable Energy Reviews* **2016**, *62*, 1063–1071. https://doi.org/10.1016/j.rser.2016.04.054

[45] Ruhul, A. M.; Kalam, M. A.; Masjuki, H. H.; Fattah, I. M. R.; Reham, S. S.; Rashed, M. M. State of the art of biodiesel production processes: A review of the heterogeneous catalyst. *RSC Advances* **2015**, *5*(122), 101023–101044. https://doi.org/10.1039/c5ra09862a

[46] Giakoumis, E. G. A statistical investigation of biodiesel physical and chemical properties, and their correlation with the degree of unsaturation. *Renewable Energy* **2013**, *50*, 858–878. https://doi.org/10.1016/j.renene.2012.07.040

[47] Abdullah, R. F.; Rashid, U.; Ibrahim, M. L.; Hazmi, B.; Alharthi, F. A.; Nehdi, I. A. Bifunctional nano-catalyst produced from palm kernel shell via hydrothermal-assisted carbonization for biodiesel production from waste cooking oil. *Renewable and Sustainable Energy Reviews* **2021**, *137*(May 2020), 110638. https://doi.org/10.1016/j.rser.2020.110638

[48] Alam, M. A.; Deng, L.; Ngatcha, A. D. P.; Fouegue, A. D. T.; Wu, J.; Zhang, S.; Zhao, A.; Xiong, W.; Xu, J. Biodiesel production from microalgal biomass by Lewis acidic deep eutectic solvent catalysed direct transesterification. *Industrial Crops and Products* **2023**, *206*(May), 117725. https://doi.org/10.1016/j.indcrop.2023.117725